

QUANTITATIVE ANALYSIS OF A CLASS OF SUBSURFACE CRACKS USING SHEAROGRAPHY AND FINITE ELEMENT MODELING

Leland D. Melvin and Brooks A. Childers
NASA Langley Research Center
Hampton, Virginia 23681

James P. Fulton
Analytical Services and Materials Inc.
107 Research Drive
Hampton, Virginia 23666

INTRODUCTION

The application of a full field non-contacting measurement system for nondestructively evaluating (NDE) subsurface flaws in structures has been conducted using Electronic Shearography. Shearography has primarily been used as a qualitative tool for locating areas of stress concentration caused by anomalies in materials[1-4]. NASA has been applying optical techniques such as these to NDE inspection of aircraft lap joint integrity, composite material defects, and pressure vessel quality assurance. This paper examines a special class of defects manufactured in thin metal panels and serves as a testbed for interpreting the displacement gradients produced on a simple well-characterized sample with known defects. Electrode discharge machining (EDM) notches were cut into panels to simulate subsurface cracks. Shearography was used to determine the detectability of subsurface cracks ranging in size from 0.8 mm to 25.4 mm fabricated in both steel and aluminum test panels. Finite element modeling was used to verify and quantify experimental results obtained in these tests. Very good agreement existed between both the experimental and predicted displacement models.

THEORETICAL CONSIDERATIONS

Shearography fringes are directly related to the derivatives of surface motion. This derivative nature of shearography fringes complicates their interpretation. Thus, while performing the reported experiments, the underlying motions governing the behavior of the fringes naturally came into question. In particular, the fringes appeared asymmetric and an explanation was sought. A simple model for shearography fringes and surface deformation was employed to aid fringe interpretation.

The equations derived by Hung [1] account for arbitrary placement of the laser source and the camera. In practice, perpendicular illumination and viewing are arranged which isolates the out of plane deformations of the surface. With this arrangement, the system displays contours of constant out-of-plane displacement derivative. Perpendicular illumination and viewing is arranged to simultaneously simplify fringe interpretation and surface illumination. The out-of-plane deformations may have many causes. They can only be interpreted to have consequences relevant to the mechanical state of the surface when

knowledge of the material characteristics and boundary conditions are available. A typical fringe pattern intensity distribution $I(x,y)$ obtained in this experiment (with near perpendicular illumination and viewing, neglecting speckle noise and system magnification) is given by

$$I(x,y) \propto \cos\left(\frac{\Delta(x,y)}{2}\right) \quad (1)$$

where $\Delta(x,y)$ is the deformation-induced optical path length change between adjacent surface locations as a function of surface coordinates (x,y) . For shearing in the x direction, the optical path length change is related to the out of plane displacement derivative

$$\frac{\partial w(x,y)}{\partial x}$$

and the shear distance δx by

$$\Delta(x,y) = \frac{4\pi}{\lambda} \delta x \frac{\partial w(x,y)}{\partial x} \quad (2)$$

where λ is the laser wavelength. According to equation (1) fringe nulls are given by the condition

$$\Delta(x,y) = (2N + 1)\pi \quad (3)$$

where $N = \pm 0, 1, 2, \dots$ represents the order of the fringe null. Therefore, from equations (2) and (3), the change in the out of plane displacement derivative required to pass to the next fringe order is








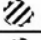
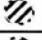



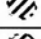

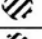
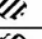


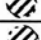
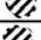
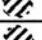



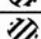
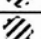
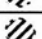









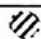
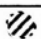


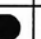

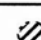
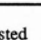

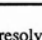
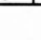



$$\frac{\lambda}{2\delta x}$$

It is apparent that the sensitivity for shearography can be adjusted by altering either the wavelength or the shear distance. Surface deformation along the x direction could be computed by appropriate successive integrations but for this study only the fringe count was measured to see if a useful correlation with crack length and strain could be found.

EXPERIMENTAL SETUP

A large test matrix of steel and aluminum panels with varying size subsurface defects were tensile loaded and the out-of-plane displacement gradients were measured using a Laser Technology Incorporated Electronic Shearography 9100 system. An MTS 810 load frame operated in stroke control was used to apply a uniform tensile load orthogonal to the horizontal notch made in each 1 mm thick by 15 x 15 cm² panel. One shearogram was recorded every 2.54 μ m of displacement applied to the panel. Loading was repeated until the fringes were no longer resolvable. Table 1 shows the test matrix used for both steel and aluminum specimens. Shearograms were captured and digitally stored using a standard 512 x 512 pixel CCD camera and a Perceptics frame grabber board all incorporated into a Macintosh fx computer. The camera and optics were modified to incorporate either the 1°, or 1/8° degree birefringent shearing crystal with either the normal (N) or zoom (Z) lens. A 30 mW 632.8 μ m wavelength Helium-Neon laser illuminated the surface of each panel as shown in Fig 1.

Table 1. Test Matrix for A1 Panel.

		Crack Length (mm)					
		25.4	12.7	6.4	3.2	1.6	0.8
Shearing Configuration	N1°X						
	N1°Y						
	Z1°X						
	Z1°Y						
	N ₈ ^{1°} X						
	N ₈ ^{1°} Y						
	Z ₈ ^{1°} X						
	Z ₈ ^{1°} Y						
		 Tested	 Unresolved				

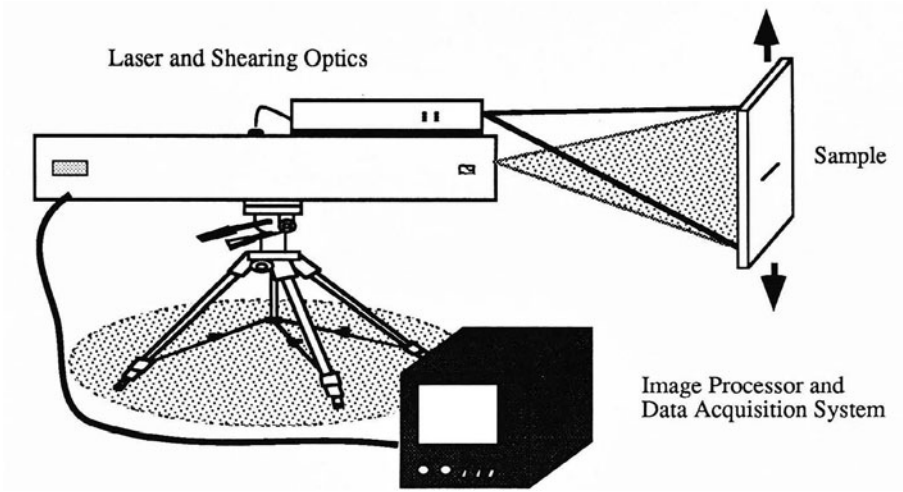


Fig. 1. Shearographic Experimental Setup.

MODELING AND RESULTS

A major focus of this work was to correlate the observed shearographic fringe patterns with important mechanical features, such as displacement, stress and strain fields, associated with the deformation of the sample. To quantify the experimental results a finite element model (FEM) was constructed using a commercial FEM software package, COSMOS™, to simulate the deformation of the samples.

Fig. 2 below illustrates the mesh used in the model. Using symmetry only the lower left hand quarter of the actual panel was modeled. The quarter panel was meshed with 2000 8-node brick elements. Symmetric boundary conditions were imposed on both the upper and right hand portions of the mesh. The rectangular region at the bottom of the figure indicates where the hydraulic grips used in the experimental setup were located. The nodes located in this part of the mesh were used to impose the displacements similar to those generated by the grips. Thus, both a tensile loading (-y direction) and a compressive loading (-z direction) were incorporated. Subsurface cracks were modeled by allowing nodes on the back set of elements along the crack length to move in the -y direction.

An example of the characteristic deformation pattern is shown in Fig. 3. When the sample is pulled the nodes along the crack region move further than the attached nodes and, as a result, cause a dimple in the plate which produces a significant out-of-plane displacement. To correlate the model with the experiments the resulting displacement field was used to compute an associated gradient field. The maximum (in absolute value) surface gradient was used together with (2) and (3) to verify that the number of fringes predicted by the FEM was equivalent to the number observed in experiments. The results show good agreement between the model and experiment. The results for a 12.7 mm and 3.175 mm crack are shown in Fig. 4.

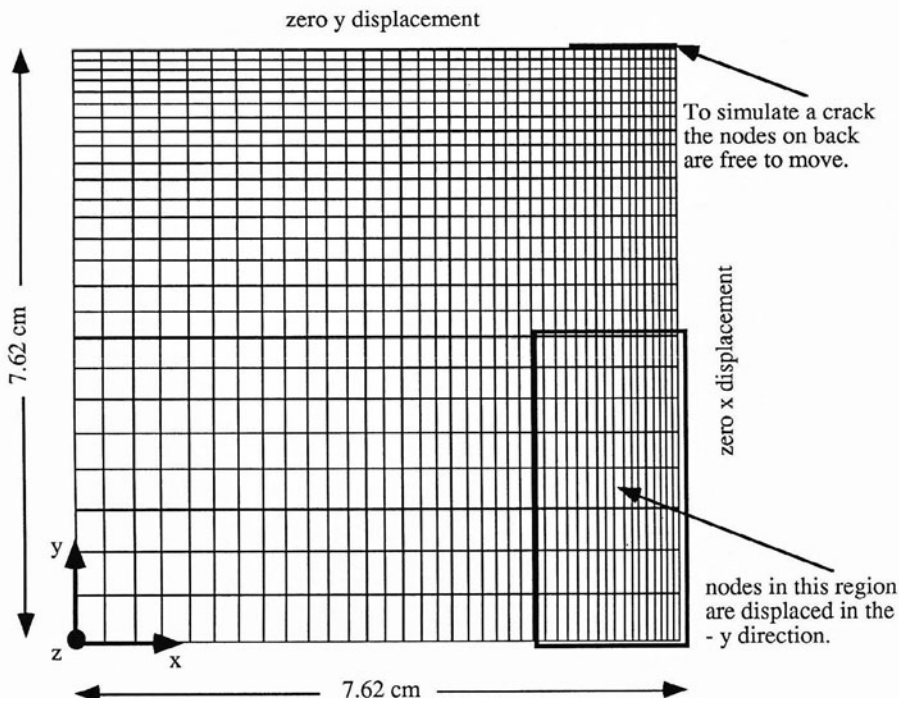


Fig. 2 Finite element mesh showing 1/4 model of panel

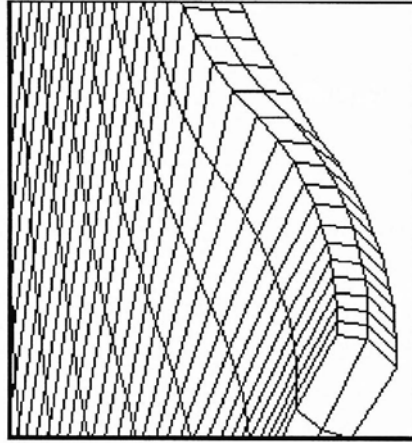


Fig. 3 Deformed plot showing out-of-plane buckling around crack region for 1/4 panel

The post-processor used with the FEM code did not allow us to arbitrarily pick where the contours appeared, consequently, a quantitative comparison between the experimental fringe patterns and those predicted by FEM could not be done at this time. However, it was possible to qualitatively compare the fringes produced by each. Fig. 5 shows FEM data for two load levels. The FEM fringes in Fig. 5 display the same qualitative shape as the experimental fringes in Fig. 6. Consequently, we were confident that our model was correctly predicting the deformation seen by shearography. The only problem seemed to be an unpredictable change in the background fringe, from dark to light, which did not show up in our model. This phenomena was subsequently explained as an effect due to a slight twisting of the sample and further analysis is provided below.

The surface deformation was modeled as a Gaussian distribution with a tilt in the x direction so

$$w(x,y) = \exp[-\sqrt{x^2 + y^2}] + Sx \quad (4)$$

where S is some arbitrary slope. A Gaussian distribution was chosen because the plot in Fig. 3 was close to that shape. The derivative of $w(x,y)$ was computed approximately by

$$\frac{\partial w(x,y)}{\partial x} \approx \frac{w(x - \delta x, y) - w(x, y)}{\delta x} \quad (5)$$

By varying the tilt slope S and the shear distance δx the fringe patterns experimentally obtained could be adequately simulated as shown in Fig. 6. It was discovered that the asymmetry could be attributed to a slight surface tilt during the experiment and did not indicate a problem with the test specimens or adversely effect the fringe count measurements. Using the fact that our FEM was in good agreement with the experiment we were then able to assign numerical values for the maximum stress and strain in the sample as a function of fringe numbers. The maximum stress which occurred at the crack tips and the maximum strain which occurred in the middle of the panel are both shown in Fig. 7. Furthermore, it was also possible to determine the size of the crack from the fringe data. The FEM model showed that the maximum gradients occurred very near the crack tips, thus, to obtain an approximate crack length we simply measured the distance between centers of the two bull's-eye patterns in the shearographic fringes. The results are plotted in Fig. 8 and are in relatively good agreement with the actual crack length.

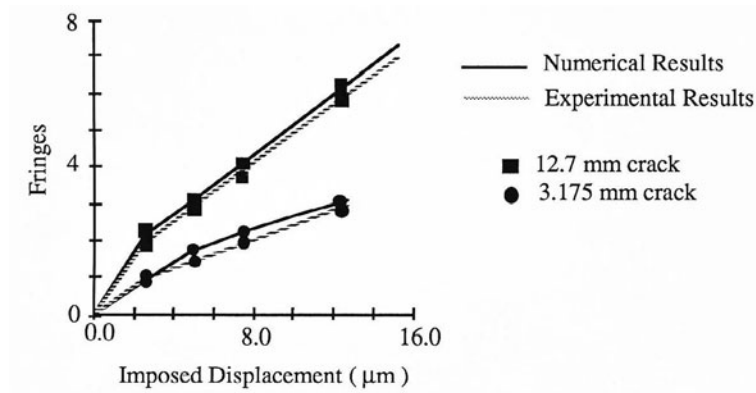


Fig. 4 Numerical and experimental results for two aluminum panels with crack lengths of 12.7 and 3.175 mm

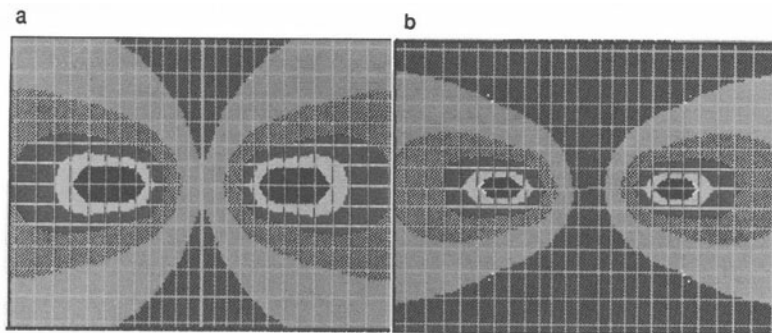


Fig. 5 Finite element model of aluminum panel with 12.7 mm subsurface crack a) displaced 7.62 μm b) displaced 10.16 μm

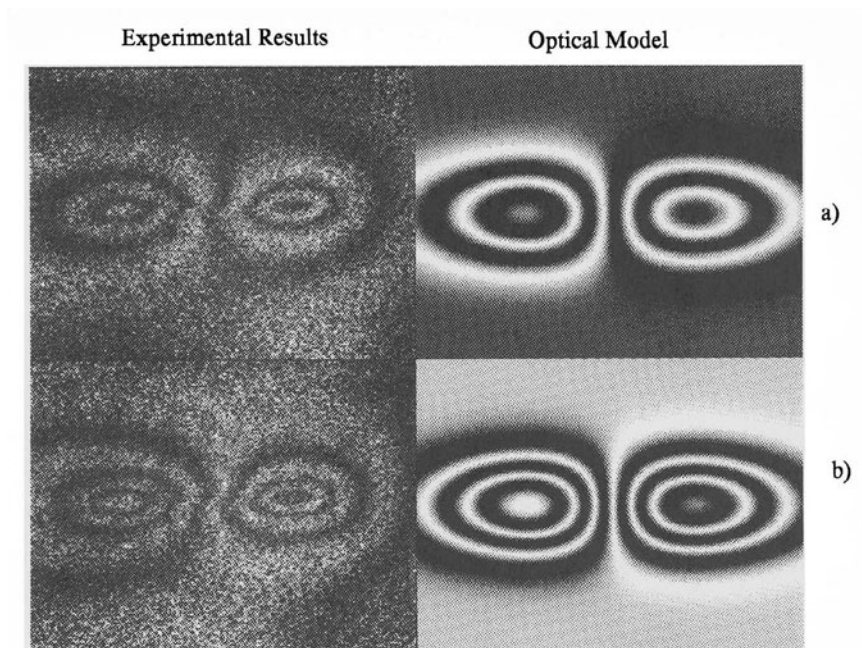


Fig. 6 Experimental and optical modeling of aluminum panel with 12.7 mm subsurface crack a) displaced 7.62 μm b) displaced 10.16 μm

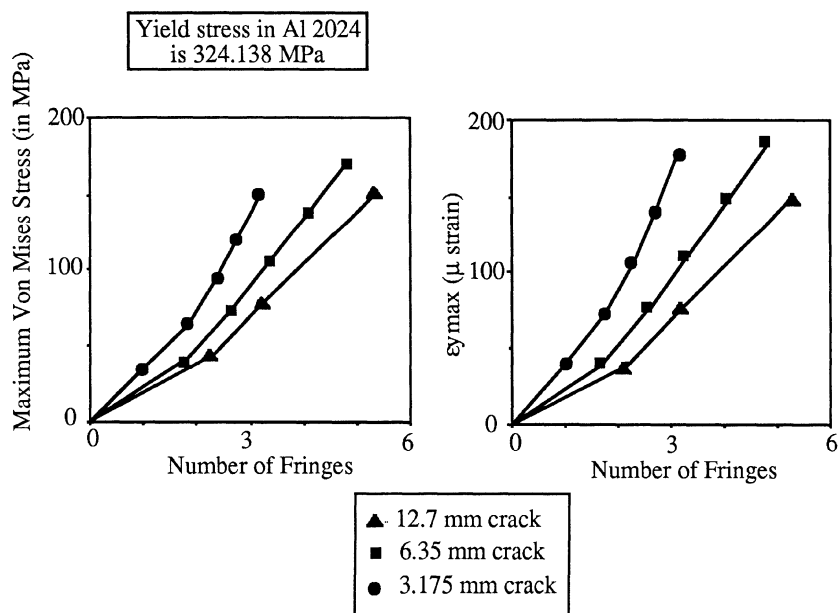


Fig. 7 Maximum stress and strain plots for aluminum panel

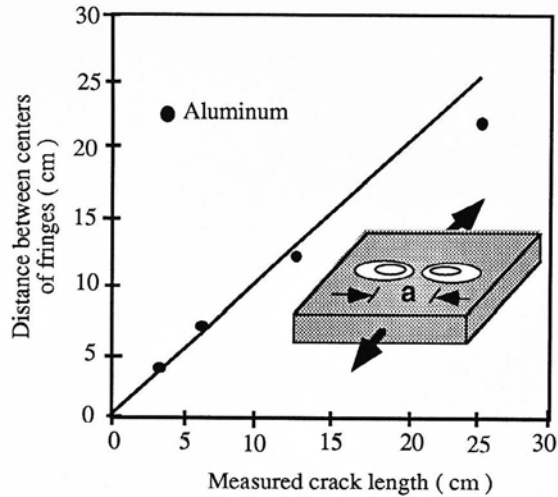


Fig. 8 Experimental and actual crack lengths

CONCLUSIONS

Electronic Shearography was used to detect subsurface flaws in thin metal panels. The smallest crack size of length 3.2 mm was detected using a 70 mm zoom lens with a 1° shearing crystal. Optical and finite element modeling was performed and agreed very well with experimental results. Good agreement was shown between the measured crack length and the distance between the shearogram double bull's-eye centers. Assignment of fringes to FEM data allowed for quantification and determination of maximum stress and strain plots for the material.

ACKNOWLEDGMENTS

This work was supported by NASA's Office of Aerospace, Exploration and Technology under RTR 538-02-11-01.

REFERENCES

1. Y. Y. Hung, and C. Y. Liuang, "Image-shearing camera for direct measurement of surface strains," *Applied Optics* 18(7), pp 1046 - 1051 (1979)
2. M. Owner-Petersen, "Digital Speckle Pattern Shearing Interferometry (DSPI). Limitations and Prospects," *Proc. Hologram Interferometry and Speckle Metrology*, pp 150-157 November (1990)
3. Y. Y. Hung *Speckle Metrology*, pp 51 - 71, Academic Press, NY, (1978)
4. Y. Y. Hung, "Shearography: a new optical method for strain measurement and nondestructive testing," *Opt. Eng.*, pp. 391 - 395 (May/June, 1982)